

Hyperfine excitation of SH⁺ by H

François Lique¹, Alexandre Zanchet^{2,3}, Niyazi Bulut⁴, Javier R. Goicoechea², and Octavio Roncero²

¹ LOMC - UMR 6294, CNRS-Université du Havre, 25 rue Philippe Lebon, BP 1123 - 76 063 Le Havre cedex, France; e-mail: francois.lique@univ-lehavre.fr

² Instituto de Física Fundamental, CSIC, C/ Serrano, 123, 28006 Madrid, Spain

³ Departamento de Química Física, Facultad de Ciencias Químicas, Universidad de Salamanca, 37008 Salamanca, Spain

⁴ Firat University, Department of Physics, 23169 Elazığ, Turkey

Received ; accepted

ABSTRACT

Context. SH⁺ is a surprisingly widespread molecular ion in diffuse interstellar clouds. There, it plays an important role triggering the sulfur chemistry. In addition, SH⁺ emission lines have been detected at the UV-illuminated edges of dense molecular clouds, so-called photo-dissociation regions (PDRs), and toward high-mass protostars. An accurate determination of the SH⁺ abundance and of the physical conditions prevailing in these energetic environments relies on knowing the rate coefficients of inelastic collisions between SH⁺ molecules and hydrogen atoms, hydrogen molecules, and electrons.

Aims. In this paper, we derive SH⁺-H fine and hyperfine-resolved rate coefficients from the recent quantum calculations for the SH⁺-H collisions, including inelastic, exchange and reactive processes.

Methods. The method used is based on the infinite order sudden approach.

Results. State-to-state rate coefficients between the first 31 fine levels and 61 hyperfine levels of SH⁺ were obtained for temperatures ranging from 10 to 1000 K. Fine structure-resolved rate coefficients present a strong propensity rule in favour of $\Delta j = \Delta N$ transitions. The $\Delta j = \Delta F$ propensity rule is observed for the hyperfine transitions.

Conclusions. The new rate coefficients will help significantly in the interpretation of SH⁺ spectra from PDRs and UV-irradiated shocks where the abundance of hydrogen atoms with respect to hydrogen molecules can be significant.

Key words. ISM: Molecules, Molecular data, Molecular processes

1. Introduction

Submillimeter emission lines from the ground rotational state of SH⁺ were first detected toward W3 IRS5 high-mass star-forming region with Herschel/HIFI (Benz et al. 2010). In parallel, and using APEX telescope, Menten et al. (2011) detected rotational absorption lines produced by SH⁺ in the low-density ($n_{\text{H}} \lesssim 100 \text{ cm}^{-3}$) diffuse clouds in the line of sight toward the strong continuum source SgrB2(M), in the Galactic Center. Despite the very endothermic formation route of this hydride ion (for a review see Gerin et al. 2016), subsequent absorption measurements of multiple lines of sight with Herschel demonstrated the ubiquitous presence of SH⁺ in diffuse interstellar clouds (Godard et al. 2012).

SH⁺ rotational lines have been also detected in emission toward the Orion Bar photo-dissociation region (PDR) (Nagy et al. 2013), a strongly UV-irradiated surface of the Orion molecular cloud (e.g., Goicoechea et al. 2016). In warm and dense PDRs ($n_{\text{H}} \gtrsim 10^5 \text{ cm}^{-3}$) like the Bar, SH⁺ forms by exothermic reactions of S⁺ with vibrationally excited H₂ (with $v \geq 2$, see details in Agúndez et al. 2010; Zanchet et al. 2013, 2019). High angular resolution images taken with ALMA shows that SH⁺ arises from a narrow layer at the edge of the PDR, the photodissociation front that separates the atomic from the molecular gas (Goicoechea et al. 2017). In these PDR layers, the abundance of hydrogen atoms is comparable to that of hydrogen molecules, that are continuously being photodissociated. Both H and H₂, together with electrons (arising from the ionization of carbon atoms, see e.g., Cuadrado et al. 2019) drive the collisional ex-

citation of molecular rotational levels and atomic fine-structure levels.

In addition to PDRs, the SH⁺ line emission observed toward massive protostars likely arises from the UV-irradiated cavities of their molecular outflows (Benz et al. 2010, 2016). In these UV-irradiated shocks, the density of hydrogen atoms can be high as well. All in all, the molecular abundances and physical conditions in these ambients where atomic and molecular hydrogen can have comparable abundances are not well understood.

In the ISM, molecular abundances are derived from molecular line modeling. Assuming local thermodynamic equilibrium (LTE) conditions in the interstellar media with low densities is generally not a good approximation, as discussed by Roueff & Lique (2013). Hence, the population of molecular levels is driven by the competition between collisional and radiative processes. It is then essential to determine accurate collisional data between the involved molecules and the most abundant interstellar species, which are usually electrons and atomic and molecular hydrogen, in order to obtain reliably modeled spectra.

The computation of collisional data for the SH⁺ started recently. First, R-matrix calculations combined with the adiabatic-nuclei-rotation and Coulomb-Born approximations was used to compute electron-impact rotational rate coefficients and hyperfine resolved rate coefficients were deduced using the infinite-order-sudden approximation (Hamilton et al. 2018). Then, time-independent close-coupling quantum scattering calculations are employed by Dagdigian (2019) to compute hyperfine-resolved rate coefficients for (de-)excitation of SH⁺ in collisions with both para- and ortho-H₂.

Collisional data with atomic hydrogen are much more challenging to compute because of the possible reactive nature of the SH⁺-H collisional system. However, recently, we overcame this difficult problem and presented quantum mechanical calculations of cross sections and rate coefficients for the rotational excitation of SH⁺ by H, including the reactive channels (Zanchet et al. 2019) using new accurate potential energy surfaces.

Unfortunately, it was not possible to include the fine and hyperfine structure of the HS⁺(³Σ⁻) molecule in the quantum dynamical calculations, whereas they are resolved in the astronomical observations leading the new set of data difficult to use in astrophysical applications.

The aim of this work is to use the quantum state-to-state rate coefficients for the HS⁺(³Σ⁻)-H inelastic collisions to generate a new set of fine and hyperfine resolved data that can be used in radiative transfer models. The paper is organized as follows : Sec. II provides a brief description theoretical approach. In Sec. III, we present the results. Concluding remarks are drawn in Sec. IV.

2. Computational methodology

2.1. Potential energy surfaces

The collisions between SH⁺(X³Σ⁻) and H(²S) can take place on two different potential energy surfaces (PESs), the ground quartet (⁴A'') and doublet (²A'') electronic states of the H₂S⁺ system. In this work, we used the H₂S⁺ quartet and doublet potential energy surfaces (PESs), that were previously generated by Zanchet et al. (2019).

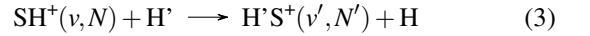
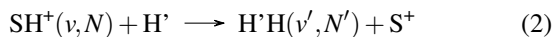
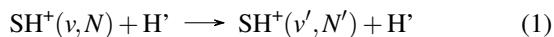
Briefly, the state-average complete active space (SA-CASSCF) method (Werner & Knowles 1985) was employed to calculate the first ⁴A'' together with the two first ²A' and the three first ²A'' electronic states. The obtained state-average orbitals and multireference configurations were then used to calculate both the lowest ⁴A'' and ²A'' states energies with the internally contracted multireference configuration interaction method (ic-MRCI) (Werner & Knowles 1988) and Davidson correction (Davidson 1975). For both sulfur and hydrogen atoms, the augmented correlation-consistent quintuple zeta (aug-cc-pV5Z) basis sets were used and all calculations were done using the MOLPRO suite of programs (Werner et al. 2012). These energies have then been fitted using the GFIT3C procedure (Aguado & Paniagua 1992; Aguado et al. 1998).

Both PESs exhibit completely different topographies. The ⁴A'' electronic state do not present any minimum out of the van der Waals wells in the asymptotic channels and does not present any barrier to SH⁺ + H → H₂ + S⁺ reaction. This reaction is exothermic on this surface and reactive collisions are likely to occur in competition with the inelastic collisions.

On the other hand, the ²A'' state presents a deep insertion HSH well and does not present any barrier neither. For this state, in contrast with the previous case, the SH⁺ + H → H₂ + S⁺ reaction is endothermic and only inelastic collisions can occur (pure or involving H exchange).

2.2. Time independent and Wave Packet calculations

During a collision between SH⁺ and H, three processes compete: the inelastic (1), reactive (2) and exchange (3) processes:



where v and N designate the vibrational and rotational levels, respectively, of the molecule (SH⁺ or H₂ when the reaction occurs). Only collisions with SH⁺ molecules in their ground vibrational state $v = 0$ are considered in this work. Therefore, the vibrational quantum number v will be omitted hereafter.

The spin-orbit couplings between the different H₂S⁺ were ignored and the collision on the ground quartet and doublet electronic states were studied separately. Because of their different topography, the dynamical calculations were treated differently on the two PESs.

The reaction dynamics on the ⁴A'' state has been studied with a time-independent treatment based on hyperspherical coordinates. On this PES, the SH⁺ + H → H₂ + S⁺ collision is a barrierless and exothermic reaction for which it has been shown (Zanchet et al. 2019) that the reactivity is large ($k > 10^{-10}$ cm³ s⁻¹), even at low temperatures. Hence, the competition between all the three processes (inelastic, exchange and reactivity) is taken into account rigorously. We used the ABC reactive code of Skouteris et al. (2000) to carry out close coupling calculations of the reactive, inelastic and exchange cross sections. The cross sections were obtained following the approach described in Tao & Alexander (2007) and recently used to study the rotational excitation of HeH⁺ (Desrousseaux & Lique 2020) by H.

We computed the cross sections for the first 13 rotational levels of the SH⁺ molecule ($0 < N < 12$) for collisional energy ranging from 0 to 5000 cm⁻¹ and for all values of the total angular momentum J leading to a non-zero contribution in the cross sections. More details about the scattering calculations can be found in Zanchet et al. (2019).

The ground doublet (²A'') electronic states exhibit a large well depth. Then, time-independent treatment is not usable and the dynamics was studied from a quantum wave-packet method using the MAD-WAVE3 program Zanchet et al. (2009). On this electronic state, the reactive channels are largely endothermic and are not open at the collisional energies considered in this work.

The inelastic and exchange cross sections on the ²A'' state were calculated using the usual partial wave expansion as

$$\begin{aligned} \sigma_{\alpha, N \rightarrow \alpha', N'}(E_k) &= \frac{\pi}{k^2} \frac{1}{2N+1} \sum_{J=0}^{J_{\max}} \sum_{\Omega, \Omega'} (2J+1) \\ &\quad \times P_{\alpha v N \Omega \rightarrow \alpha' v' N' \Omega'}^J(E_k) \end{aligned} \quad (4)$$

where J is the total angular momentum quantum number, and Ω, Ω' are the projections of the total angular momentum on the reactant and product body-fixed z-axis, respectively. $\alpha = I, \alpha' = I$ or E denotes the arrangement channels, inelastic or exchange. $k^2 = 2\mu_r E_k / \hbar^2$ is the square of the wave vector for a collision energy E_k , and $P_{\alpha v N \Omega \rightarrow \alpha' v' N' \Omega'}^J(E_k)$ are the transition probabilities, *i.e.* the square of the corresponding S-matrix elements. We computed the cross sections from the $N = 0$ rotational states to the first 13 rotational levels of the SH⁺ molecule ($0 < N' < 12$) for collisional energy ranging from 0 to 5000 cm⁻¹. Because of the high computational cost of these simulations, they are only performed for $J=0, 10, 15, 20, 25, 30, 40, 50, \dots, 110$, while for intermediate J values they are interpolated using a uniform J -shifting approximation as recently used for the OH⁺-H and CH⁺-H collisional systems Werfelli et al. (2015); Bulut et al. (2015). The convergence analysis and the parameters used in the propagation for each of the two PESs used are described in detail in Zanchet et al. (2019).

For both sets of calculations, since the two rearrangement channels, inelastic and exchange, yields to the same products, the corresponding cross sections are summed for the doublet and quartet states independently. Finally, the cross sections for each of the two electronic states are summed with the proper degeneracy factor to give the total collision cross sections as

$$\sigma_{N \rightarrow N'}(E_k) = \frac{2}{3} \sigma_{N \rightarrow N'}^{S=3/2}(E_k) + \frac{1}{3} \sigma_{N \rightarrow N'}^{S=1/2}(E_k). \quad (5)$$

As seen in Zanchet et al. (2019), the magnitude of the excitation cross sections obtained on the doublet states are larger than that on the quartet states, because of the both, the non reactive character of the collision and of the deep well that favor inelastic collisions.

From the total collision cross sections $\sigma_{N \rightarrow N'}(E_k)$, one can obtain the corresponding thermal rate coefficients at temperature T by an average over the collision energy (E_k):

$$k_{N \rightarrow N'}(T) = \left(\frac{8}{\pi \mu k_B^3 T^3} \right)^{\frac{1}{2}} \times \int_0^{\infty} \sigma_{N \rightarrow N'}(E_k) E_k \exp(-E_k/k_B T) dE_k \quad (6)$$

where k_B is Boltzmann's constant and μ the reduced mass. The cross sections calculations carried out up to kinetic energy of 5000 cm⁻¹ allowed computing rate coefficients for temperatures ranging from 10 to 1000 K.

In all these calculations, the spin-rotation couplings of SH⁺ have not been included, and therefore the present set of rate coefficients cannot be directly used to model interstellar SH⁺ spectra where the fine and hyperfine structure is resolved.

2.3. Infinite order sudden (IOS) calculations

In this section, we describe how the state-to-state fine and hyperfine rate coefficients for the SH⁺-H collisional system were computed using IOS methods (Goldflam et al. 1977; Faure & Lique 2012) using the above $k_{0 \rightarrow N'}(T)$ rate coefficients as "fundamental" rate coefficients (those out of the lowest level)

For SH⁺ in its ground electronic ³Σ⁻ state, the molecular energy levels can be described in the Hund's case (b) limit¹. The fine structure levels are labeled by Nj , where j is the total molecular angular momentum quantum number with $j = N + S$. S is the electronic spin. For molecules in a ³Σ⁻ state, $S = 1$. Hence, three kinds of levels ($j = N - 1$, $j = N$ and $j = N + 1$) exist, except for the $N = 0$ rotational level which is a single level.

The hydrogen atom also possesses a non-zero nuclear spin ($I = 1/2$). The coupling between I and j results in a splitting of each level into two hyperfine levels (except for the $N = 1, j = 0$ level which is split into only one level). Each hyperfine level is designated by a quantum number F ($F = I + j$) varying between $|I - j|$ and $I + j$.

Using the IOS approximation, rate coefficients among fine structure levels can be obtained from the $k_{0 \rightarrow L}(T)$ "fundamental" rate coefficients using the following formula (e.g.

Corey & McCourt 1983):

$$k_{Nj \rightarrow N'j'}^{IOS}(T) = (2N + 1)(2N' + 1)(2j' + 1) \sum_L \left(\begin{matrix} N' & N & L \\ 0 & 0 & 0 \end{matrix} \right)^2 \left\{ \begin{matrix} N & N' & L \\ j' & j & S \end{matrix} \right\}^2 \times k_{0 \rightarrow L}(T) \quad (7)$$

where $\left(\begin{matrix} & & \\ & & \end{matrix} \right)$ and $\left\{ \begin{matrix} & & \\ & & \end{matrix} \right\}$ are respectively the "3-j" and "6-j" symbols. In the usual IOS approach, $k_{0 \rightarrow L}(T)$ is calculated for each collision angle. Here, however, we use the $k_{0 \rightarrow L}(T)$ rate coefficients of Eq. (6) obtained with a more accurate quantum method.

The hyperfine resolved rate coefficients can also be obtained from the fundamental rate coefficients as follow Faure & Lique (2012):

$$k_{NjF \rightarrow N'j'F'}^{IOS}(T) = (2N + 1)(2N' + 1)(2j + 1)(2j' + 1) \times (2F' + 1) \sum_L \left(\begin{matrix} N' & N & L \\ 0 & 0 & 0 \end{matrix} \right)^2 \left\{ \begin{matrix} N & N' & L \\ j' & j & S \end{matrix} \right\}^2 \left\{ \begin{matrix} j & j' & L \\ F' & F & I \end{matrix} \right\}^2 \times k_{0 \rightarrow L}(T) \quad (8)$$

In addition, we note that the fundamental excitation rates $k_{0 \rightarrow L}(T)$ were in practice replaced by the de-excitation fundamental rates using the detailed balance relation:

$$k_{0 \rightarrow L}(T) = (2L + 1)k_{L \rightarrow 0}(T) \quad (9)$$

where

$$k_{L \rightarrow 0}(T) = k_{0 \rightarrow L}(T) \frac{1}{2L + 1} e^{\frac{\epsilon_L}{k_B T}} \quad (10)$$

ϵ_L is the energies of the rotational levels L .

This procedure was indeed found to significantly improve the results at low temperatures due to important threshold effects.

The fine and hyperfine splittings of the rotational states are of a few cm⁻¹ and of a few 0.001 cm⁻¹, respectively and can be neglected compared to the collision energy at $T > 30 - 50$ K so that the present approach is expected to be reasonably accurate for all the temperature range considered in this work. Lique et al. (2016) have investigated the accuracy of the IOS approach in the case of OH⁺-H collisions. It was shown to be reasonably accurate (within a factor of 2), even at low temperature so that we can anticipate a similar accuracy for the present collisional system. In addition, we note that with the present approach, some fine and hyperfine rate coefficients are strictly zero. This selection rule is explained by the "3-j" and "6-j" Wigner symbols that vanish for some transitions. Using a more accurate approach, these rate coefficients will not be strictly zero but will generally be smaller than the other rate coefficients.

3. Results

Using the computational methodology described above, we have generated fine and hyperfine resolved rate coefficients for the SH⁺-H collisional system using the doublet and quartet pure rotational rate coefficients in order to provide the astrophysical community with the first set of data for the SH⁺-H collisional system. In all the calculations, we have considered all the SH⁺ energy levels with $N, N' \leq 10$ and we have included in the calculations all the fundamental rate coefficients with $L \leq 12$. The complete set of (de)excitation rate coefficients is available on-line from the LAMDA (Schöier et al. 2005) and BASECOL (Dubernet et al. 2013) websites.

¹ For ³Σ⁻ electronic ground state molecules, the energy levels are usually described in the intermediate coupling scheme (Gordy & Cook 1984; Lique et al. 2005). However, the use of IOS scattering approach implies to use the Hund's case (b) limit.

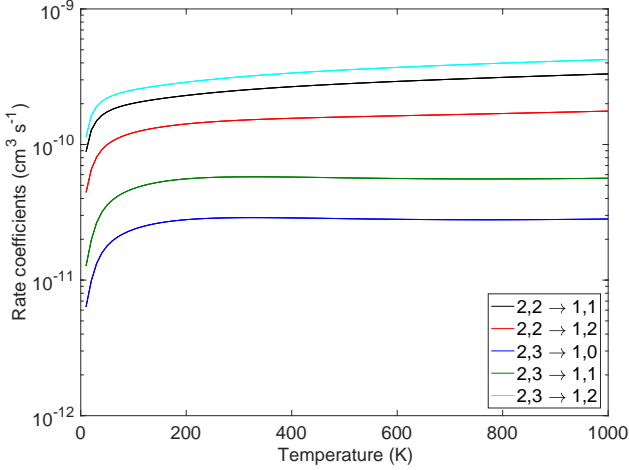


Fig. 1. Temperature variation of the fine structure resolved de-excitation rate coefficients for the SH⁺ molecule in collision with H for selected $N = 2, j \rightarrow N' = 1, j'$ transitions.

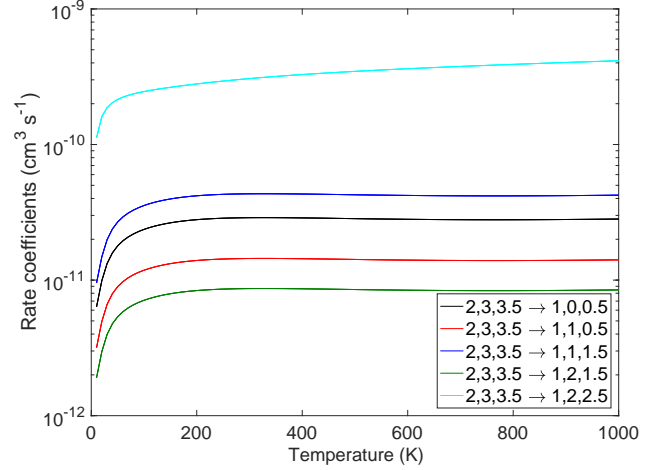


Fig. 2. Temperature variation of the hyperfine structure resolved de-excitation rate coefficients for the SH⁺ molecule in collision with H for the $N = 2, j = 3, F = 3.5 \rightarrow N' = 1, j', F'$ transitions.

3.1. Fine and hyperfine structure excitation

The thermal dependence of the fine structure resolved state-to-state SH⁺-H rate coefficients is illustrated in Fig. 1 for selected $N = 2, j \rightarrow N' = 1, j'$ transitions.

The temperature variation of the de-excitation rate coefficients is relatively smooth except at low temperature ($T < 50\text{K}$) where they increase rapidly. The weak temperature dependence of the rate coefficients (except at low temperature) could have been anticipated, on the basis of Langevin theory for ion-neutral interactions.

A strong propensity rule exists for $\Delta j = \Delta N$ transitions. Such $\Delta j = \Delta N$ propensity rule was predicted theoretically (Alexander & Dagdigian 1983) and is general for molecules in the $^3\Sigma^-$ electronic state. It was also observed previously for the O₂(X³Σ⁻)-He (Lique 2010), NH(X³Σ⁻)-He (Tobola et al. 2011) or OH⁺-H (Lique et al. 2016) collisions

Figure 2 presents the temperature variation of the hyperfine structure resolved state-to-state SH⁺-H rate coefficients for selected $N = 2, j = 3, F = 3.5 \rightarrow N' = 1, j', F'$ transitions.

For $\Delta j = \Delta N$ transitions, we have a strong propensity rule in favor of $\Delta j = \Delta F$ hyperfine transitions. This trend is the usual trend for open-shell molecules (Alexander 1985; Dumouchel et al. 2012; Kalugina et al. 2012; Lique et al. 2016). For $\Delta j \neq \Delta N$ transitions, it is much more difficult to find a clear propensity rule. The final distribution seems to be governed by two rules: the rate coefficients show propensity in favor of $\Delta j = \Delta F$ transitions, but are also proportional to the degeneracy ($2F' + 1$) of the final hyperfine level as already found for CN-para-H₂ system (Kalugina et al. 2012).

3.2. Comparison with SH⁺-H₂ rate coefficients

Then, we compare the new SH⁺-H rate coefficients with those reported recently for the hyperfine excitation of SH⁺ by H₂ (Dagdigian 2019). The SH⁺ molecule has been observed in media where both atomic and molecular hydrogen are significant colliding partners and this comparison should allow evaluating the impact of the different collisional partners.

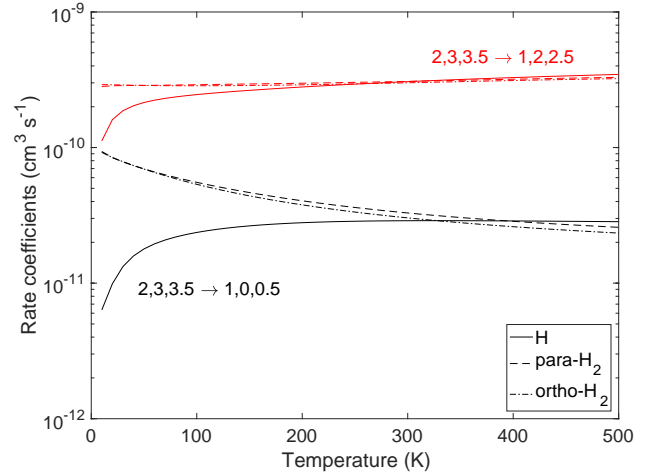


Fig. 3. Comparison between SH⁺-H and SH⁺-H₂ (both para- and ortho-H₂) rate coefficients for a selected number of hyperfine ($N = 2, j = 3, F = 3.5 \rightarrow N' = 1, j', F'$) transitions.

In Fig. 3, we compare the SH⁺-H and SH⁺-H₂ (both para- and ortho-H₂) rate coefficients for a selected number of transitions.

In astrophysical applications, when collisional data are not available, it is very common to derive collisional data from collisional rate coefficients calculated for the same molecule in collision with another colliding partner. Such approach (Lique et al. 2008), consist in assuming that the excitation cross-sections are similar for both colliding systems and that the rate coefficients differ only by a scaling factor due to the reduced mass which appears in Eq. 6. Hence, the following scaling relationship can be used:

$$k^{\text{H}} \simeq 1.4 \times k^{\text{H}_2} \quad (11)$$

One can see that, at low temperatures, the rate coefficients for collisions with H do not have the highest magnitude as expected from the scaling relationships. They can even be one order of magnitude weaker. We also note that the differences between H

and H₂ rate coefficients depend on the transitions and on the temperature leading to the impossibility of extrapolating accurate H collisional data from H₂ collisional data, or the reverse. Hence, it confirms that it is unrealistic to estimate unknown collisional rate coefficients by simply applying a scaling factor to existing rate coefficients. This result was previously observed for water (Daniel et al. 2015) and ammonia (Bouhafs et al. 2017).

However, when the temperature increases, the agreement gets better and scaling techniques would lead to a reasonable estimate of the H or H₂ rate coefficients for temperatures above 500 K.

4. Summary and Conclusion

The fine and hyperfine excitation of SH⁺ by H have been investigated. We have obtained fine and hyperfine resolved rate coefficients for transitions involving the lowest levels of SH⁺ for temperatures ranging from 10 to 1000 K. Fine structure resolved rate coefficients present a strong propensity rules in favor of $\Delta j = \Delta N$ transition. The $\Delta j = \Delta F$ propensity rule is observed for the hyperfine transitions.

As a molecule that can be observed from ground-based observatories (Müller et al. 2014), in the Milky Way and beyond (Muller et al. 2017), we expect that these new data will significantly help in the accurate interpretation of SH⁺ rotational emission spectra from dense PDRs and massive proto-stars, enable this molecular ion to act as tracer of the energetics of these regions, and of the first steps of the sulfur chemistry.

Acknowledgements. We acknowledge the French-Spanish collaborative project PICS (Ref. PIC2017FR7). F.L. acknowledges financial support from the European Research Council (Consolidator Grant COLLEXISM, grant agreement 811363), the Institut Universitaire de France and the Programme National "Physique et Chimie du Milieu Interstellaire" (PCMI) of CNRS/INSU with INC/INP co-funded by CEA and CNES. The research leading to these results has received funding from MICIU under grants No. FIS2017-83473-C2 and AYA2017-85111-P. N.B. acknowledges the computing facilities by TUBITAK-TRUBA. This work was performed using HPC resources from GENCI-CINES (Grant A0070411036).

References

- Aguado, A. & Paniagua, M. 1992, *J. Chem. Phys.*, 96, 1265
 Aguado, A., Tablero, C., & Paniagua, M. 1998, *Comput. Physics Commun.*, 108, 259
 Agúndez, M., Goicoechea, J. R., Cernicharo, J., Faure, A., & Roueff, E. 2010, *ApJ*, 713, 662
 Alexander, M. H. 1985, *Chem. Phys.*, 92, 337
 Alexander, M. H. & Dagdigian, P. J. 1983, *J. Chem. Phys.*, 79, 302
 Benz, A. O., Bruderer, S., van Dishoeck, E. F., et al. 2016, *A&A*, 590, A105
 Benz, A. O., Bruderer, S., van Dishoeck, E. F., et al. 2010, *A&A*, 521, L35
 Bouhafs, N., Rist, C., Daniel, F., et al. 2017, *Monthly Notices of the Royal Astronomical Society*, 470, 2204
 Bulut, N., Lique, F., & Roncero, O. 2015, *Journal of Physical Chemistry A*, 119, 12082
 Corey, G. C. & McCourt, F. R. 1983, *J. Phys. Chem.*, 87, 2723
 Cuadrado, S., Salas, P., Goicoechea, J. R., et al. 2019, *A&A*, 625, L3
 Dagdigian, P. J. 2019, *MNRAS*, 487, 3427
 Daniel, F., Faure, A., Dagdigian, P. J., et al. 2015, *MNRAS*, 446, 2312
 Davidson, E. R. 1975, *J. Comput. Phys.*, 17, 87
 Desrousseaux, B. & Lique, F. 2020, *J. Chem. Phys.*, 152, 074303
 Dubernet, M.-L., Alexander, M. H., Ba, Y. A., et al. 2013, *A&A*, 553, A50
 Dumouchel, F., Klos, J., Toboła, R., et al. 2012, *J. Chem. Phys.*, 137, 114306
 Faure, A. & Lique, F. 2012, *MNRAS*, 425, 740
 Gerin, M., Neufeld, D. A., & Goicoechea, J. R. 2016, *ARA&A*, 54, 181
 Godard, B., Falgarone, E., Gerin, M., et al. 2012, *A&A*, 540, A87
 Goicoechea, J. R., Cuadrado, S., Pety, J., et al. 2017, *A&A*, 601, L9
 Goicoechea, J. R., Pety, J., Cuadrado, S., et al. 2016, *Nature*, 537, 207
 Goldflam, R., Kouri, D. J., & Green, S. 1977, *J. Chem. Phys.*, 67, 5661
 Gordy, W. & Cook, R. L. 1984, *Microwave molecular spectra (Wileys and sons)*
 Hamilton, J. R., Faure, A., & Tennyson, J. 2018, *MNRAS*, 476, 2931

- Kalugina, Y., Lique, F., & Klos, J. 2012, *MNRAS*, 422, 812
 Lique, F. 2010, *J. Chem. Phys.*, 132, 044311
 Lique, F., Bulut, N., & Roncero, O. 2016, *MNRAS*, 461, 4477
 Lique, F., Spielfiedel, A., Dubernet, M. L., & Feautrier, N. 2005, *J. Chem. Phys.*, 123, 134316
 Lique, F., Toboła, R., Klos, J., et al. 2008, *A&A*, 478, 567
 Menten, K. M., Wyrowski, F., Belloche, A., et al. 2011, *A&A*, 525, A77
 Müller, H. S. P., Goicoechea, J. R., Cernicharo, J., et al. 2014, *A&A*, 569, L5
 Müller, S., Müller, H. S. P., Black, J. H., et al. 2017, *A&A*, 606, A109
 Nagy, Z., Van der Tak, F. F. S., Ossenkopf, V., et al. 2013, *A&A*, 550, A96
 Roueff, E. & Lique, F. 2013, *Chem. Rev.*, 113, 8906
 Schöier, F. L., van der Tak, F. F. S., van Dishoeck, E. F., & Black, J. H. 2005, *A&A*, 432, 369
 Skouteris, D., Castillo, J. F., & Manolopoulos, D. E. 2000, *Comput. Phys. Commun.*, 133, 128
 Tao, L. & Alexander, M. H. 2007, *J. Chem. Phys.*, 127, 114301
 Toboła, R., Dumouchel, F., Klos, J., & Lique, F. 2011, *J. Chem. Phys.*, 134, 024305
 Werfelli, G., Halvick, P., Honvault, P., Kerkeni, B., & Stoecklin, T. 2015, *J. Chem. Phys.*, 143, 114304
 Werner, H.-J. & Knowles, P. J. 1985, *J. Chem. Phys.*, 82, 5053
 Werner, H.-J. & Knowles, P. J. 1988, *J. Chem. Phys.*, 89, 5803
 Werner, H.-J., Knowles, P. J., Knizia, G., Manby, F. R., & Schütz, M. 2012, *WIREs Comput Mol Sci*, 2, 242
 Zanchet, A., Agúndez, M., Herrero, V. J., Aguado, A., & Roncero, O. 2013, *AJ*, 146, 125
 Zanchet, A., Lique, F., Roncero, O., Goicoechea, J. R., & Bulut, N. 2019, *A&A*, 626, A103
 Zanchet, A., Roncero, O., González-Lezana, T., et al. 2009, *J. Phys. Chem. A*, 113, 14488